ELSEVIER

Chemical Engineering Journal 121 (2006) 115–123

Chemical Engineering Journal

www.elsevier.com/locate/cej

Partial oxidation of methane over Ni/Ce-Ti-O catalysts

Yuan Zhang [a], Zengxi Li [b], Xuebing Wen [a], Yuan Liu [a,*]

[a] *School of Chemical Engineering and Technology, Tianjin University, Tianjin 300072, China*
[b] *Graduate School of the Chinese Academy of Sciences, Beijing 100049, China*

Received 8 September 2005; received in revised form 28 March 2006; accepted 5 May 2006

Abstract

Partial oxidation of methane (POM) was studied in this work. The supported nickel catalysts were prepared by the coprecipitation–impregnation method. The influence of the molar ratio of Ce/Ti, the calcination temperature, and the content of active component were investigated during the process of preparation. The results show that the mixed oxides of the Ce-Ti-O-supported Ni catalysts exhibited high catalytic activity and stability. Among the catalysts investigated, the highest catalytic activity was observed over 10 wt.% $NiO/Ce_{0.50}Ti_{0.50}O_2$-700 °C which showed excellently stable performance during 100 h on stream at 750 °C. The catalysts were characterized by DTA/TG, BET, XRD, and TPR. XRD and TPR results confirmed that the NiO in all catalysts was highly dispersed. There was no NiO but only $NiTiO_3$ in the NiO/TiO_2 catalyst, due to the reaction between NiO and TiO_2. $NiTiO_3$ is harder to be reduced to Ni^0 than NiO. The addition of CeO_2 could form a solid solution of Ce-Ti-O, which was able to restrain the reaction between NiO and TiO_2 and improve the storage capacity and mobility of oxygen. It was shown that Ni^0 reduced from $NiTiO_3$ was active for the POM reaction.

Keywords: Partial oxidation of methane; POM; Ceria; Titania; Solid solution; Hydrogen production

1. Introduction

In recent years, fuel cells have received a great deal of attention [1], particularly from the automotive industry [2]. Proton exchange membrane fuel cell (PEMFC), as a candidate for near-future power generation applications, is particularly suited to automotive applications primarily because its relatively low operating temperature, efficiency, and high power density make it comparable to existing internal combustion technology [3].

Hydrogen resource is an important system in PEMFC. There are many routes for hydrogen production [4]. As a result of various difficulties for hydrogen storage, more attention has been paid to on-board hydrogen production. Partial oxidation of methane (POM) is a suitable hydrogen production process [5] because it has rapid reaction velocity, low consumption of energy, and low investment.

The catalyst design is the main point for the POM process. Two groups of catalysts have been studied for partial oxidation of methane: noble metal-based catalysts and Ni-based catalysts. The former includes Pt [6], Pd [7], Rh [8,9], Ru [10] and Ir [11], and Rh and Ru have the highest activity and stability [12]. Noble metal-based catalysts seem to be more active for the POM reaction than Ni-based catalysts, but the high-cost limits their industrial utilization.

Ni-based catalysts have been investigated for several years [13–18] because of their appreciable catalytic activity, good stability, and low price. Since the support can exert a great influence on the type of carbonaceous species formed by the methane interaction with the metallic particles dispersed on its surface, it has an intense effect on catalyst performance. The usual supports include oxides such as Al_2O_3, MgO, SiO_2, CaO, Y_2O_3, La_2O_3, ZrO_2, CeO_2, TiO_2, HfO_2, $MgMAlO_x$ spinel, $CaTiO_3$ perovskite, H-Y zeolite, and their mixed oxides [13]. Diskin et al. [14] prepared supported-Ni catalysts with different supports. Ni/SiO_2 showed the highest activity and selectivity for CO formation, Ni/Al_2O_3 the worst. Wu et al. [15] investigated the deactivation of methane to syngas over the Ni/TiO_2 catalyst. They found that deactivation is due largely to the oxidation of Ni^0 to $NiTiO_3$ rather than by carbon deposition in the POM reaction. Zhu and Flytzani-Stephanopoulos [16] synthesized the bulk Ni-CeO_2 catalysts by the urea coprecipitation method using metal nitrates and urea. The results confirmed that 5 at.% Ni-CeO_2 catalyst showed excellent resistance to carbon deposition and stable performance during 100 h-on-stream at 650 °C. Mixed oxides-

* Corresponding author.
E-mail address: yuanliu@tju.edu.cn (Y. Liu).

1385-8947/$ – see front matter © 2006 Elsevier B.V. All rights reserved.
doi:10.1016/j.cej.2006.05.014

supported catalysts often show great performance. Roh et al. [17] prepared several catalysts for the POM reaction. They found that Ni/Ce-ZrO_2 catalyst had higher activity than Ni/CeO_2 or Ni/ZrO_2. They explained that the presence of ceria in the catalyst had beneficial effects on enhancing the concentration of highly mobile oxygen species and the ceria-zirconium solid solution led to a lower reduction temperature. Takeguchi et al. [18] discovered the activity of the NiO/CeO_2-ZrO_2 catalysts increased with an increase of oxygen storage capacity of the CeO_2-ZrO_2 solid solutions. The NiO particles having strong interaction with the support showed high stability for partial oxidation of methane, while the NiO particles having weak interaction produced a large amount of coke.

CeO_2, a stable fluorite-type oxide, has a good oxygen storage capacity [19]. It can be reduced in oxygen deficient conditions while oxidized in oxygen sufficient conditions. Ceria has been examined as a promoter of both the activity and selectivity of Ni catalysts for the POM reaction [20]. Titanium and zirconium are both IVB elements, and Ti^{4+} has a smaller ionic radius than Zr^{4+}. That indicates it may have great effect on the mobile oxygen species after Ti^{4+} gets into the ceria crystal lattice. Researchers have discovered that ceria-titania compound oxides have special redox behavior [21,22]. They were used in supported-CuO catalysts [23].

Among Ni-based catalysts, NiO/CeO_2-TiO_2 compound oxides catalysts have been rarely reported. In this work, we have studied a CeO_2-TiO_2-supported Ni catalyst for POM, and it is found that the active component in Ni/CeO_2-TiO_2 and Ni/CeO_2-ZrO_2 is different.

2. Experimental

2.1. Catalyst preparation

The compound oxide supports were prepared by coprecipitation. 0.5 mol L^{-1} $Ce(NO_3)_3$ solution and 0.3 mol L^{-1} $TiCL_4$ solution were mixed in proportion. The mixed solution and 2 mol L^{-1} ammonia were dropped together while stirring vigorously and maintained at pH 10, aging for 24 h after the reaction. The precipitate was washed three times with 200 mL deionized water and twice with 100 mL ethanol, and then dried in an oven at 80 °C for 24 h, producing a precursor. The supported-Ni catalyst was prepared by impregnating the precursor with an aqueous solution of $Ni(NO_3)_2$. It was deposited overnight to disperse it well, then dried in an oven at 80 °C for 24 h again. This was followed by pre-calcining in air at 350 °C for 2 h, then at a proper temperature for 4 h.

The expression of catalyst stands for, taking 10 wt.% NiO/$Ce_{0.50}Ti_{0.50}O_2$-800 °C as an example, the catalyst with a NiO content is 10 wt.%, a molar ratio of Ce/Ti is 0.50:0.50, and calcined at 800 °C.

2.2. Catalytic reaction

Catalytic activity tests were carried out in a fixed tubular quartz micro-reactor (500 mm length, 8 mm i.d.) operated at atmospheric pressure. A 100 mg catalyst sample was used for all runs. Catalyst was first reduced in 5 vol.% H_2–Ar at 650 °C for 30 min. Then the reactor system was flushed in nitrogen for 10 min. The reactant gas of 16 vol.% CH_4, 10 vol.% O_2 in nitrogen was then introduced to the reactor. O_2 was taken in slight excess over the stoichiometry to compensate its deficiency caused by total combustion. Gas flow rates were controlled at GHSV = 55,200 mL h^{-1} g_{cat}^{-1} by mass flow meters. The reactant and product mixtures were analyzed by a SP-2100 gas chromatograph (GC) equipped with a thermal conductivity detector and two columns. A carbon sieve GDX-502 (packed column, 2 m length, 4 mm i.d.) column was used to separate CO_2 and other gases (O_2, N_2, CO, and CH_4) while a molecular sieve 5A column was used to separate O_2, N_2, CO, and CH_4. Conversion of methane and selectivity of carbon monoxide and hydrogen are calculated by the following formulae:

$$X(CH_4) = \frac{(CH_4)_{in} - (CH_4)_{out}}{(CH_4)_{in}} \times 100\% \quad (1)$$

$$S(CO) = \frac{(CO)_{out}}{(CH_4)_{in} - (CH_4)_{out}} \times 100\% \quad (2)$$

$$S(H_2) = \frac{(H_2)_{out}}{2[(CH_4)_{in} - (CH_4)_{out}]} \times 100\% \quad (3)$$

2.3. Characterization technique

Specific surface areas were calculated by the BET method from N_2 adsorption isotherms, recorded at liquid nitrogen temperature on a Micromeritics apparatus model ASAP-2000.

Powder X-ray diffraction (XRD) patterns of samples were recorded on D/Max-2500 X-ray diffractometer in order to identify the different phases present in the catalyst and to determine their crystalline phases. Cu Kα radiation (λ = 0.15406 nm) was used with a power setting of 40 kV and 100 mA. (scan rate = 5° min^{-1}).

Temperature programmed reduction (TPR) of the samples was carried out in a TPR analyzer (Thermo Finnigan modeled TPDRO 1100 Series) in a 5 vol.% H_2–N_2 gas mixture with a rate of 20 mL min^{-1}. A 10 mg catalyst sample was used in each run. After being loaded into the quartz tube reactor, the sample was heated in the gas mixture from room temperature to 950 °C with a heating rate of 10 °C min^{-1}, and then maintained at 950 °C for 5 min.

Differential thermal analysis and thermo gravimetric analysis (DTA/TG, Perkin-Elmer, Pyris Diamond) were made in a dry-air atmosphere using a heating rate of 10 °C min^{-1}.

3. Results and discussion

3.1. BET surface area results

Table 1 gives the specific surface areas of catalysts prepared in various conditions. According to Table 1, the specific surface areas increase with the addition of ceria, and decrease with an increase in calcination temperature and with an increase in Ni content.

Table 1
BET surface area of different catalysts

Catalyst	BET surface area ($m^2\ g^{-1}$)
10 wt.% NiO/TiO_2-800 °C	4.0
10 wt.% $NiO/Ce_{0.25}Ti_{0.75}O_2$-800 °C	15.1
10 wt.% $NiO/Ce_{0.50}Ti_{0.50}O_2$-800 °C	19.2
10 wt.% $NiO/Ce_{0.75}Ti_{0.25}O_2$-800 °C	17.1
10 wt.% NiO/CeO_2-800 °C	28.1
10 wt.% $NiO/Ce_{0.50}Ce_{0.50}Ti_{0.50}O_2$-700 °C	37.2
10 wt.% $NiO/Ce_{0.50}Ti_{0.50}O_2$-900 °C	11.3
5 wt.% $NiO/Ce_{0.50}Ti_{0.50}O_2$-800 °C	23.5
15 wt.% $NiO/Ce_{0.50}Ti_{0.50}O_2$-800 °C	18.6

3.2. Catalytic performance

The catalytic performance of the catalysts is influenced by their preparation conditions. The molar ratio of Ce/Ti, the calcination temperature, and the content of Ni are essential parameters that should be controlled.

3.2.1. Effect of Ce/Ti ratio

10 wt.% $NiO/Ce_xTi_{1-x}O_2$ samples with different Ce/Ti ratios ($x = 0$, 0.25, 0.50, 0.75, 1) were prepared. The five catalysts were all active for the POM reaction with similar trends, as shown in Fig. 1. Conversion of CH_4 was enhanced at high-temperature and kept going up as the temperature rose. 10 wt.% $NiO/Ce_{0.50}Ti_{0.50}O_2$-800 °C exhibited the highest CH_4 conversion at the reaction temperature range of 700–800 °C. CH_4 conversion reached 95% at 800 °C, which is close to the equilibrium conversion. Table 1 shows that 10 wt.% $NiO/Ce_{0.50}Ti_{0.50}O_2$-800 had the largest specific surface area among the three $Ce_xTi_{1-x}O_2$-supported catalysts, which indicates that the high activity might be partly the result of its high specific surface area.

3.2.2. Effect of calcination temperature

10 wt.% $NiO/Ce_{0.50}Ti_{0.50}O_2$ catalysts were calcined at 700, 800, and 900 °C. The catalytic activity decreases with an increase in calcination temperature, as shown in Fig. 2. Especially at lower reaction temperature (650 °C), CH_4 conversion is 82% over catalyst calcined at 700 °C, while only 76 and 75% over catalysts calcined at 800 and 900 °C, respectively. The results in Table 1 also show that catalyst calcined at 700 °C has the largest BET surface area. The small surface area of catalysts calcined at high-temperature may lead to lower CH_4 conversion. Meanwhile, high calcination temperature might result in separation of TiO_2 from Ce-Ti solid solution (this will be discussed in Section 3.4), which may also influences the catalytic performance.

3.2.3. Effect of Ni content

Catalysts with NiO loading of 5, 10, and 15 wt.% were prepared by impregnating $Ce_{0.50}Ti_{0.50}O_2$ with $Ni(NO_3)_2$. Fig. 3 lists the results of catalytic performance measurement. As shown in Fig. 3(a), CH_4 conversion increases by 4 and 8% at 650 and 700 °C, respectively with the NiO content increasing from 5 to 10 wt.%. When NiO loading is higher than 10 wt.%, CH_4 con-

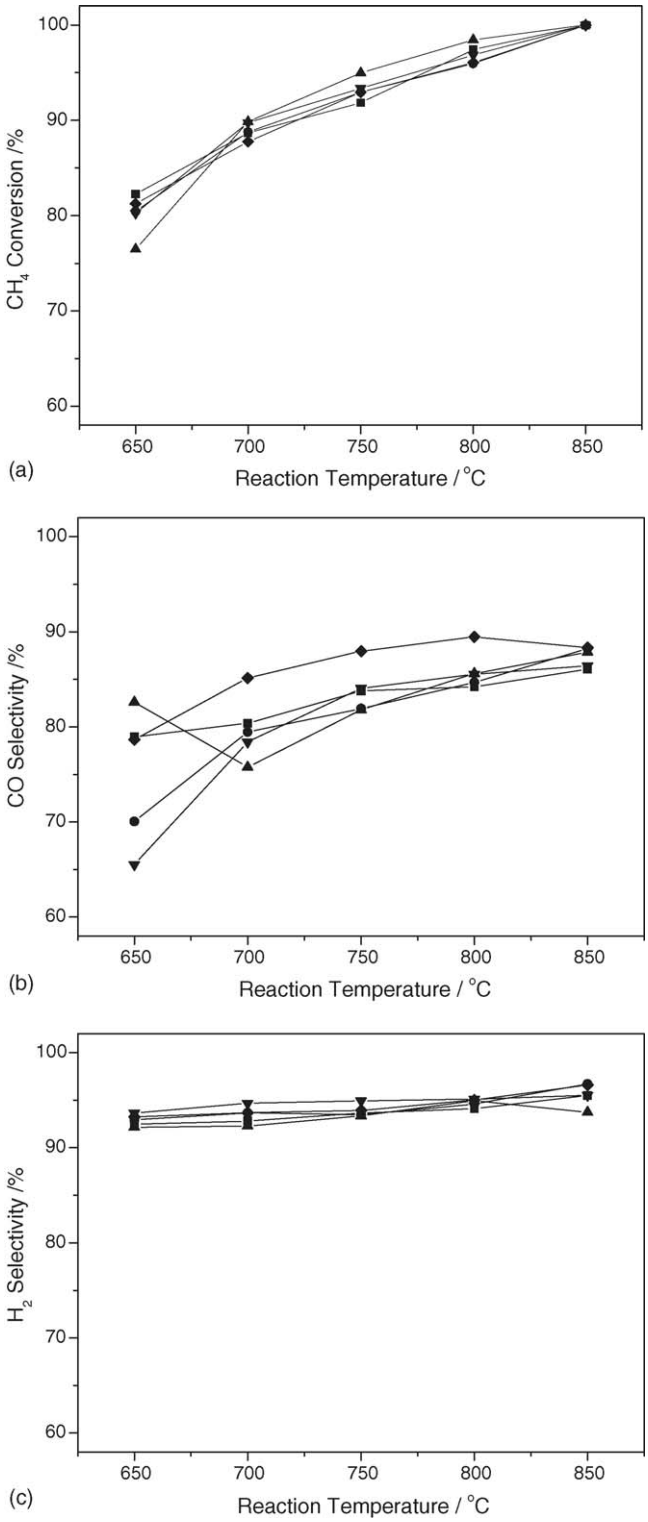

Fig. 1. Catalytic activity of 10 wt.% $NiO/Ce_xTi_{1-x}O_2$-800 °C with different Ce/Ti: (a) CH_4 conversion-temperature, (b) CO selectivity-temperature and (c) H_2 selectivity-temperature ((■)10 wt.% NiO/TiO_2-800 °C; (●) 10 wt.% $NiO/Ce_{0.25}Ti_{0.75}O_2$-800 °C; (▲) 10 wt.% $NiO/Ce_{0.50}Ti_{0.50}O_2$-800 °C; (▼) 10 wt.% $NiO/Ce_{0.75}Ti_{0.25}O_2$-800 °C; and (♦) 10 wt.% NiO/CeO_2-800 °C).

version shows a slight decrease at the reaction temperature of 650 and 700 °C. So 10 wt.% NiO loading is sufficient, more NiO has little contribution to catalytic activity for the POM reaction.

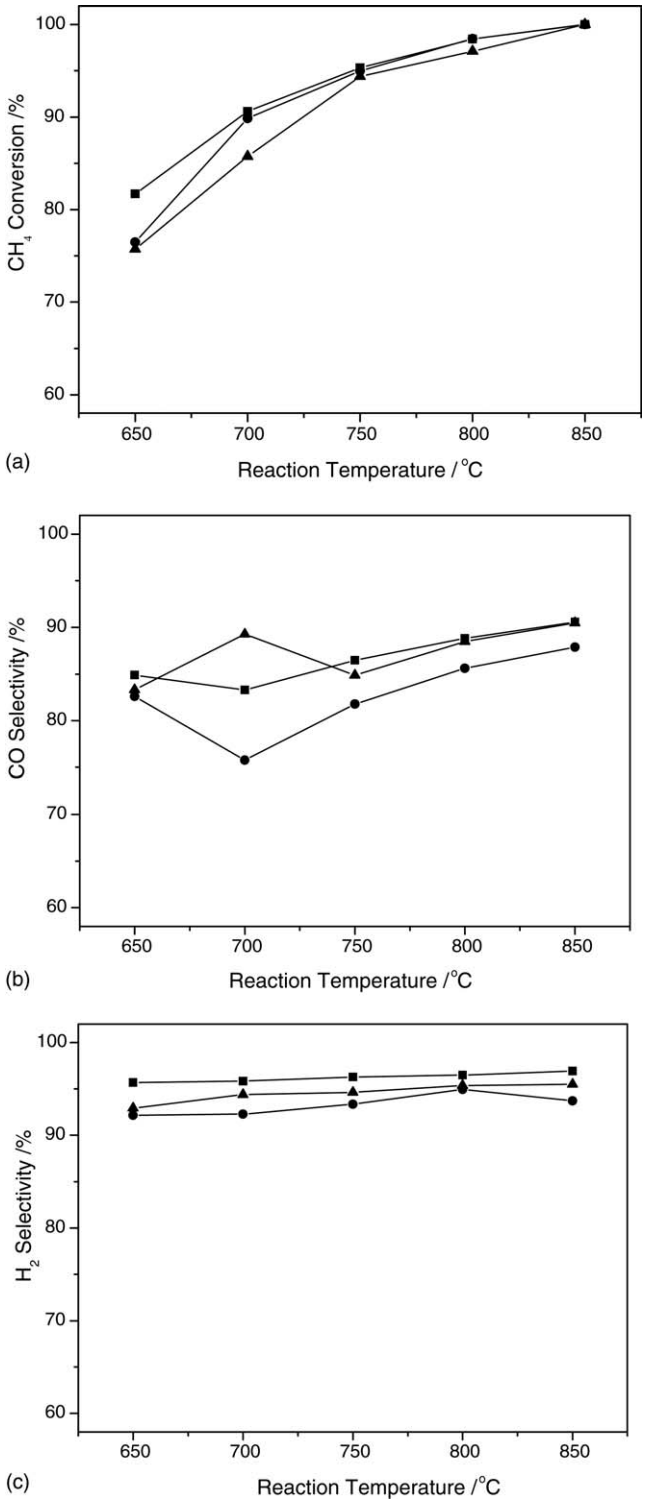

Fig. 2. Catalytic activity of 10 wt.% $NiO/Ce_{0.50}Ti_{0.50}O_2$ calcined at different temperature: (a) CH_4 conversion-temperature, (b) CO selectivity-temperature and (c) H_2 selectivity-temperature ((■) 10 wt.% $NiO/Ce_{0.50}Ti_{0.50}O_2$-700 °C; (●) 10 wt.% $NiO/Ce_{0.50}Ti_{0.50}O_2$-800 °C; and (▲) 10 wt.% $NiO/Ce_{0.50}Ti_{0.50}O_2$-900 °C).

3.3. Stability testing results

The 10 wt.% $NiO/Ce_{0.50}Ti_{0.50}O_2$-700 °C catalyst showed a very good stability at 750 °C with a CH_4/O_2 ratio of 1.6 at a GHSV of 55,200 mL h^{-1} g_{cat}^{-1}, as shown in Fig. 4. No distinct

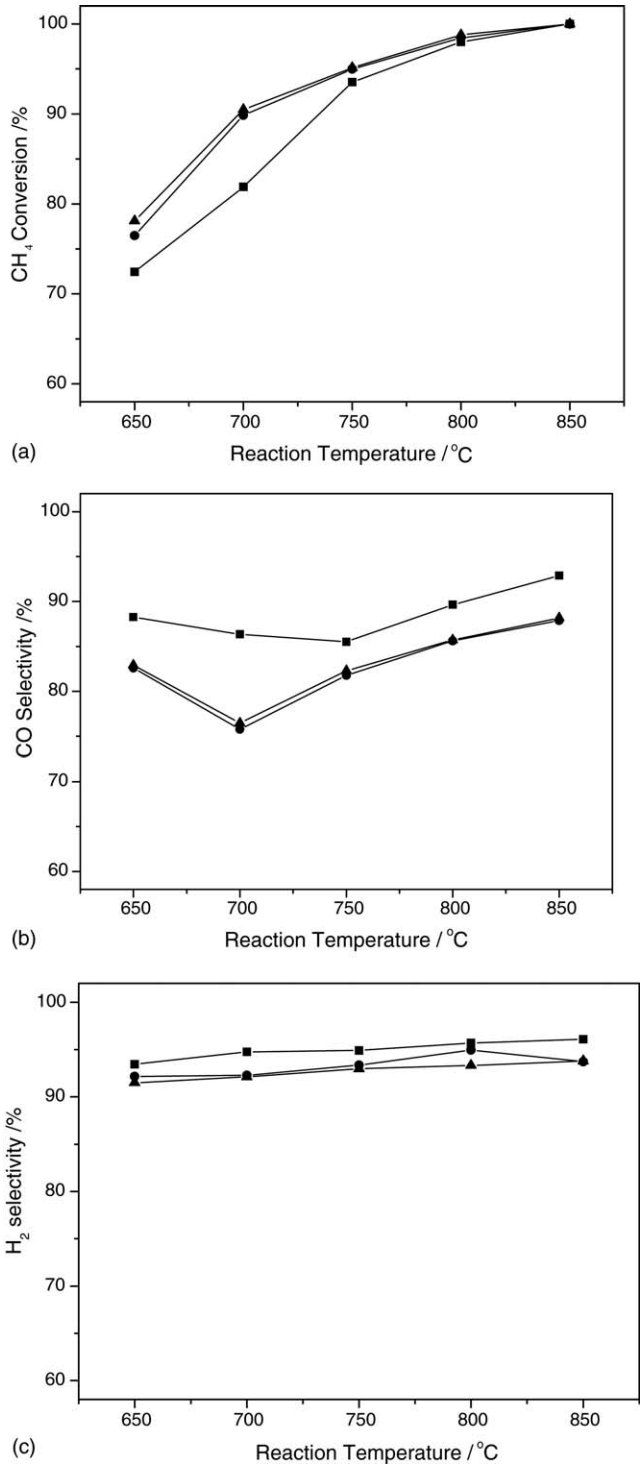

Fig. 3. Catalytic activity of $NiO/Ce_{0.50}Ti_{0.50}O_2$-800 °C with different NiO content: (a) CH_4 conversion-temperature, (b) CO selectivity-temperature and (c) H_2 selectivity-temperature ((■) 5 wt.% $NiO/Ce_{0.50}Ti_{0.50}O_2$-800 °C; (●) 10 wt.% $NiO/Ce_{0.50}Ti_{0.50}O_2$-800 °C; and (▲) 15 wt.% $NiO/Ce_{0.50}Ti_{0.50}O_2$-800 °C).

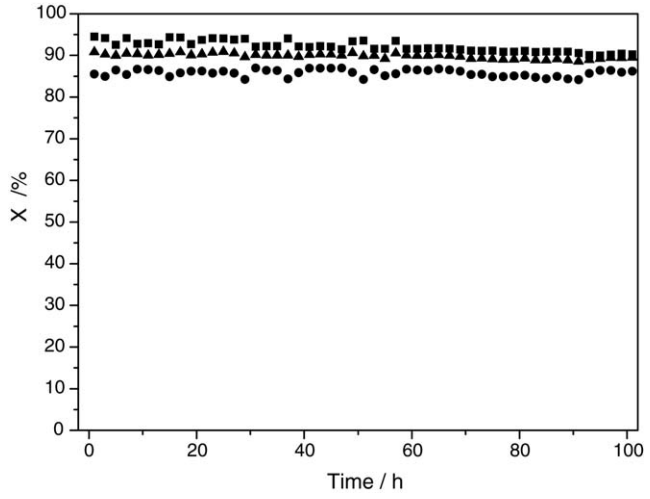

Fig. 4. Stability test of 10 wt.% NiO/$Ce_{0.50}Ti_{0.50}O_2$-700 °C at 750 °C, GHSV = 55,200 mL h^{-1} g_{cat}^{-1} and CH_4:O_2 = 1.6:1 ((■) conversion of CH_4; (●) selectivity of CO; and (▲) selectivity of H_2).

deactivation was observed during 100 h on stream. CH_4 conversion and H_2 selectivity were maintained at ~93 and ~90%, respectively.

From the catalytic performance tests, we could found that the Ni/Ce-Ti-O catalysts had excellent activity and stability for the POM reaction. Wu et al. [15] prepared supported Ni/TiO_2 catalyst, and it exhibited rapid deactivation from the start in the POM process. It indicates that the addition of ceria greatly improves the resistance to deactivation. Table 2 lists the comparison of catalytic activity of different catalysts in the literatures and this work. This implies that Ni/Ce-Ti-O is a potential catalyst for the POM reaction.

3.4. XRD results

XRD studies were performed on the calcined samples prepared in different conditions. For discerning the structure more clearly, the crystalline phases involved in each catalyst are summarized in Table 3, and Table 3 also shows the ceria lattice parameter calculated from ceria (1 1 1) reflection. Figs. 5–7 depicts the XRD patterns of all samples.

XRD patterns for catalysts with different Ce/Ti ratios are shown in Fig. 5(A–E). Discernible NiO diffraction peaks were only found in the NiO/CeO_2 sample. This indicates that no bulk NiO exists in the other catalysts. $NiTiO_3$ diffraction peaks were clearly observed in all catalysts except NiO/CeO_2. That is to say, TiO_2 addition avoids the formation of bulk NiO due to the solid-state reaction of NiO and TiO_2. No obvious TiO_2 diffraction peaks appeared in the NiO/$Ce_{0.75}Ti_{0.25}O_2$ catalysts. The CeO_2 lattice parameter in NiO/Ce-Ti-O decreases compared with that in NiO/CeO_2, as shown in Table 3. Ti^{4+} has a smaller ionic radius than Ce^{4+}. After Ti^{4+} enters the ceria crystal lattice, the CeO_2 lattice parameter should decrease. It can be seen from Table 3 that the CeO_2 lattice parameter is smaller in NiO/Ce-Ti-O compared with in NiO/CeO_2, which indicates the formation of ceria-titania solid solution. So, the smaller ceria lattice parameter, the more Ti^{4+} enters the ceria crystal lattice, the more ceria-titania solid solution forms. By combining this XRD study with the results

Table 2
Comparison of catalytic activity of different catalysts for POM reaction

Catalyst	Conversion of CH_4 (%)	Selectivity of H_2 (%)	Selectivity of CO (%)	Reactant gas	Reaction temperature (°C)	GHSV	Reference
8 wt.% Ni/TiO_2	77	93	75	CH_4:O_2 = 2:1	700	150000 h^{-1}	[15]
5 at.% Ni/Ce(La)O_x	90	–	91	3 mol% CH_4, 1.5 mol% O_2 in N_2	650	0.18 g s cm^{-3} (20000 mL h^{-1} g^{-1})	[16]
15 wt.% Ni/$CeZrO_2$	85	98	89	CH_4:O_2 = 1.875:1	750	55200 mL h^{-1} g_{cat}^{-1}	[17]
NiO(12.4)/$Ce_{0.03}Zr_{0.97}O_2$(GT)	72	83	87	10 vol.% CH_4, 5 vol.% O_2 in N_2	650	120000 L kg^{-1} h^{-1}	[18]
10 wt.% NiO/$Ce_{0.50}Ti_{0.50}O_2$-700 °C	93	90	86	16 vol.% CH_4, 10 vol.% O_2 in N_2	750	55200 mL h^{-1} g_{cat}^{-1}	This work

Table 3
The crystalline phases and ceria lattice parameter in each catalysts

Catalyst	Crystalline phases					CeO_2 lattice parameter, a (Å)[a]
	Cerianite	Anatase	Rutile	$NiTiO_3$	NiO	
10 wt.% NiO/TiO_2-800 °C	–	–	√	√	–	–
10 wt.% NiO/$Ce_{0.25}Ti_{0.75}O_2$-800 °C	√	√	√	√	–	5.413
10 wt.% NiO/$Ce_{0.50}Ti_{0.50}O_2$-800 °C	√	–	√	√	–	5.405
10 wt.% NiO/$Ce_{0.75}Ti_{0.25}O_2$-800 °C	√	–	–	√	–	5.413
10 wt.% NiO/CeO_2-800 °C	√	–	–	–	√	5.420
10 wt.% NiO/$Ce_{0.50}Ti_{0.50}O_2$-700 °C	√	–	–	√	–	5.376
10 wt.% NiO/$Ce_{0.50}Ti_{0.50}O_2$-900 °C	√	–	√	√	–	5.413
5 wt.% NiO/$Ce_{0.50}Ti_{0.50}O_2$-800 °C	√	√	√	√	–	5.402
15 wt.% NiO/$Ce_{0.50}Ti_{0.50}O_2$-800 °C	√	–	√	√	–	5.405

[a] Calculated from ceria (1 1 1) reflection from the equation $a = \sqrt{h^2 + k^2 + l^2}(\lambda/2 \sin\theta)$ [24].

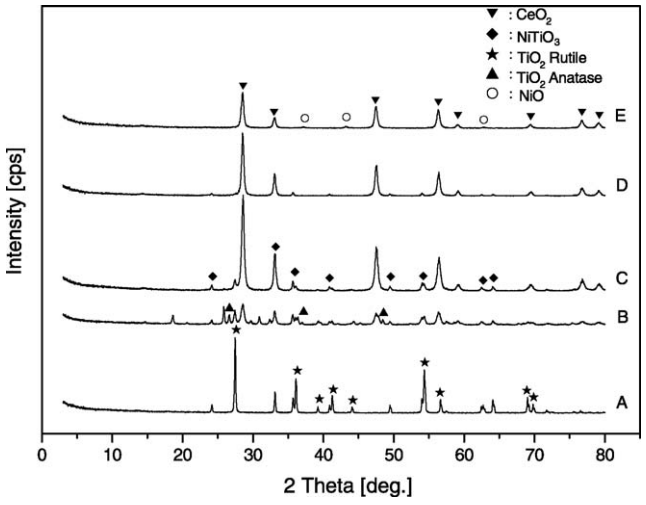

Fig. 5. XRD patterns of 10 wt.% NiO/$Ce_xTi_{1-x}O_2$-800 °C with different Ce/Ti ratio: (A) 10 wt.% NiO/TiO_2-800 °C; (B) 10 wt.% NiO/$Ce_{0.25}Ti_{0.75}O_2$-800 °C; (C) 10 wt.% NiO/$Ce_{0.50}Ti_{0.50}O_2$-800 °C; (D) 10 wt.% NiO/$Ce_{0.75}Ti_{0.25}O_2$-800 °C; and (E) 10 wt.% NiO/CeO_2-800 °C.

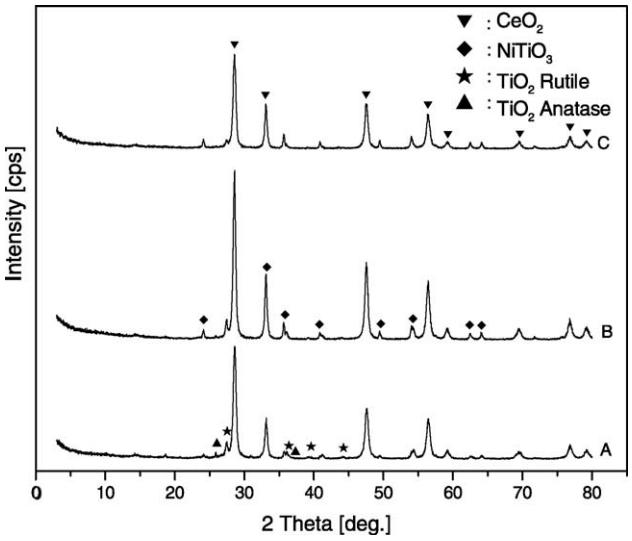

Fig. 7. XRD patterns of NiO/$Ce_{0.50}Ti_{0.50}O_2$-800 °C with different NiO content: (A) 5 wt.% NiO/$Ce_{0.50}Ti_{0.50}O_2$-800 °C; (B) 10 wt.% NiO/$Ce_{0.50}Ti_{0.50}O_2$-800 °C; and (C) 15 wt.% NiO/$Ce_{0.50}Ti_{0.50}O_2$-800 °C.

of the catalytic activity tests, it is found that the best catalyst, 10 wt.% NiO/$Ce_{0.50}Ti_{0.50}O_2$-700 °C, has the smallest ceria lattice parameter, which indicates that the correlation of ceria-titania solid solution and the catalytic activity.

Fig. 6(A–C) lists the XRD patterns of 10 wt.% NiO/$Ce_{0.50}Ti_{0.50}O_2$ calcined at 700, 800, and 900 °C. All diffraction peaks become shaper with the increase of calcination temperature. No obvious TiO_2 diffraction is present in the catalysts calcined at 700 °C, which shows that titanium is in the form of Ce-Ti-O solid solution and $NiTiO_3$. Rutile diffraction peaks are observed in catalysts calcined 800 and 900 °C. The results imply that the ceria-titania solid solution was not very stable, and titania would separate out at higher calcination temperatures. As shown in Fig. 2, catalyst calcined at 700 °C exhibited a higher activity than at 800 or 900 °C in POM.

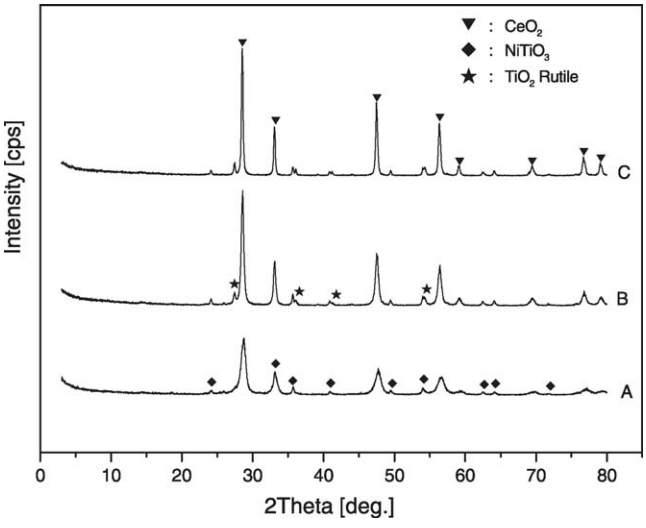

Fig. 6. XRD patterns of 10 wt.% NiO/$Ce_{0.50}Ti_{0.50}O_2$ calcined at different temperature: (A) 10 wt.% NiO-$Ce_{0.50}Ti_{0.50}O_2$-700 °C; (B) 10 wt.% NiO-$Ce_{0.50}Ti_{0.50}O_2$-800 °C; and (C) 10 wt.% NiO-$Ce_{0.50}Ti_{0.50}O_2$-900 °C.

Thus, catalytic performance may be related to the formation of ceria-titania solid solution to some extent.

Fig. 7(A–C) shows the XRD patterns of NiO/$Ce_{0.50}oTi_{0.50}O_2$-800 °C catalysts with NiO content of 5, 10, and 15 wt.%. TiO_2 diffraction peaks become weaker, while $NiTiO_3$ diffraction peaks become stronger with the increase of NiO loading. This means the solid-state reaction of NiO and TiO_2 is improved by the increase of NiO content.

3.5. TPR results

The reduction behavior of Ni-based catalysts was investigated by means of TPR. All catalysts were examined in 5 vol.% H_2 in N_2. TPR profiles of 10 wt.% NiO/$Ce_xTi_{1-x}O_2$-800 °C with different Ce/Ti ratios are shown in Fig. 8(A–E). Only one reduction peak is observed in NiO/TiO_2 at about 630 °C, which is due to the reduction of Ni^+ in bulk $NiTiO_3$ to Ni^0 [15]. At least three reduction peaks are observed for NiO/CeO_2 at temperatures of 280, 380, and 790 °C. Unsupported NiO has a reduction temperature of about 280 °C [15]. Therefore, the small peak between 260 and 300 °C in NiO/CeO_2 is assigned to bulk NiO. The peak at the temperature of about 380 °C is due to the reduction of NiO interacted with the support [15,18,25]. The small and broad peak at 790 °C is related to the partial reduction of Ce^{4+} to Ce^{3+} [15,26,27]. Three obvious reduction peaks are presented in the other three $Ce_xTi_{1-x}O_2$-supported catalysts at temperatures of 390, 650, and 800 °C. The reduction peaks near 390 °C are exhibited in Fig. 8(B–E), which is due to the reduction of NiO interacting with support, while no NiO diffraction peaks can be detected for the same samples in the XRD patterns. It indicates that NiO species are highly dispersed in these catalysts.

Though only the $NiTiO_3$ reduction peak presented itself in NiO/TiO_2, a high catalytic activity was shown over the catalysts. This shows that Ni^0 reduced from $NiTiO_3$ species could be active to the POM reaction. Wu et al. [15] studied the deactivation of Ni/TiO_2 catalyst. Rapid deactivation was observed from the

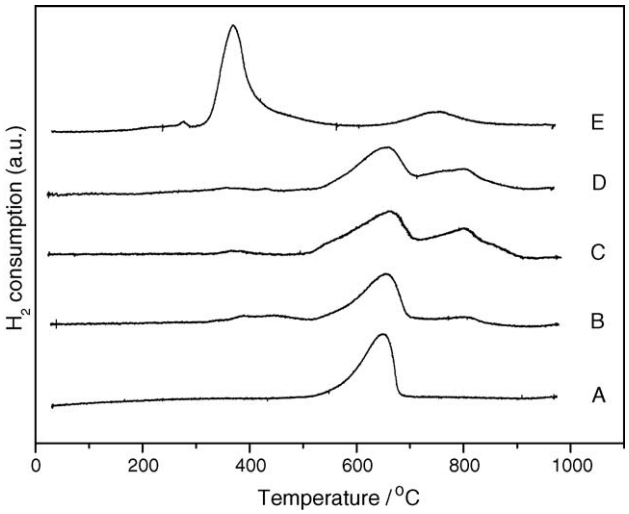

Fig. 8. TPR profiles of 10 wt.% NiO/$Ce_xTi_{1-x}O_2$-800 °C with different Ce/Ti ratio: (A) 10 wt.% NiO/TiO_2-800 °C; (B) 10 wt.% NiO/$Ce_{0.25}Ti_{0.75}O_2$-800 °C; (C) 10 wt.% NiO/$Ce_{0.50}Ti_{0.50}O_2$-800 °C; (D) 10 wt.% NiO/$Ce_{0.75}Ti_{0.25}O_2$-800 °C; and (E) 10 wt.% NiO/CeO_2-800 °C.

start in the POM process. CH_4 conversion decreased from an initial value of 76–43% after 20 h of reaction. They concluded that the formation of $NiTiO_3$ was the main reason for catalysts deactivation. That is different from our conclusion. Despite the hard reduction of $NiTiO_3$, the Ni^0 reduced from $NiTiO_3$ is still an active component for POM reaction.

Fig. 9(A–C) presents TPR profiles of 10 wt.% NiO/$Ce_{0.50}Ti_{0.50}O_2$ calcined at 700, 800, and 900 °C. At least three reduction peaks are observed for all catalysts at temperatures of about 390, 650, and 800 °C. The reduction peaks at about 390 °C become weaker as the calcination temperature of catalysts increase. This suggests that NiO interaction with the support was not stable, and the solid-state reaction between NiO and TiO_2 are improved as calcination temperature increases. Comparing these three TPR profiles, from A to C, the reduction

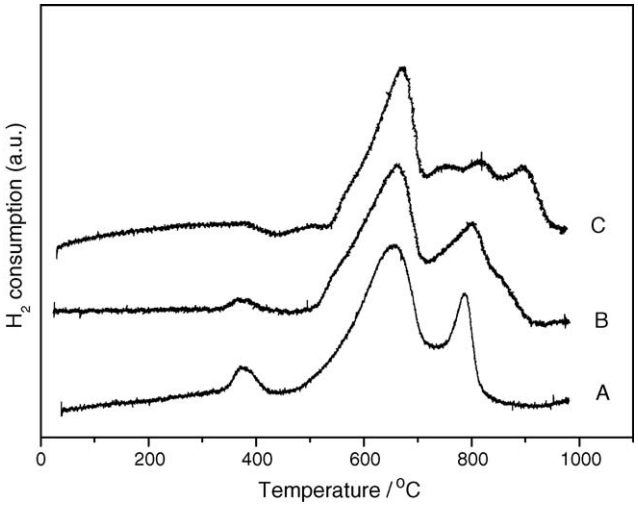

Fig. 9. TPR pattern of 10 wt.% NiO/$Ce_{0.50}Ti_{0.50}O_2$ calcined at different temperature: (A) 10 wt.% NiO/$Ce_{0.50}Ti_{0.50}O_2$-700 °C; (B) 10 wt.% NiO/$Ce_{0.50}Ti_{0.50}O_2$-800 °C; and (C) 10 wt.% NiO/$Ce_{0.50}Ti_{0.50}O_2$-900 °C.

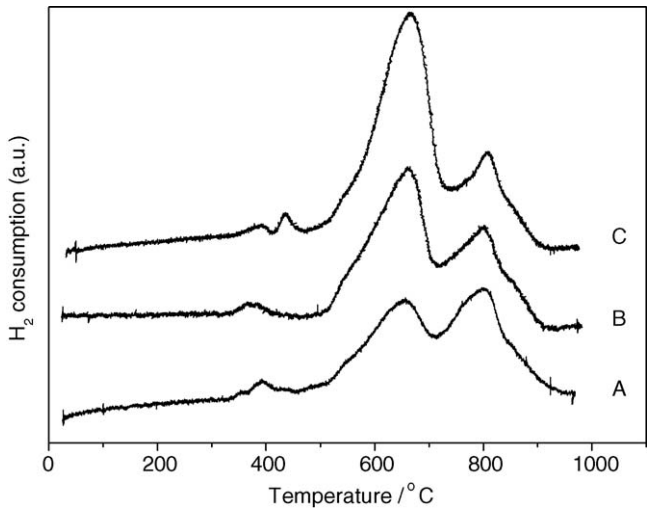

Fig. 10. TPR profiles of NiO/$Ce_{0.50}Ti_{0.50}O_2$-800 °C with different NiO content: (A) 5 wt.% NiO/$Ce_{0.50}Ti_{0.50}O_2$-800 °C; (B) 10 wt.% NiO/$Ce_{0.50}Ti_{0.50}O_2$-800 °C; and (C) 15 wt.% NiO/$Ce_{0.50}Ti_{0.50}O_2$-800 °C.

peak of 650 °C is shifted to a higher value, which indicates that the higher the calcination temperature, the stabler the $NiTiO_3$. There are also a series of weak peaks between 830 and 900 °C. These may be related to the reduction of different types of ceria-titania solid solution.

TPR profiles of NiO/$Ce_{0.50}Ti_{0.50}O_2$-800 °C with NiO loading of 5, 10, and 15 wt.% are shown in Fig. 10(A–C). The reduction area of 670 °C increases with the increase of NiO loading. This means that the increase of NiO is mainly to forming $NiTiO_3$. An unresolved peak with the maximum temperature at 420 °C is observed in the 15 wt.% NiO catalyst. This suggests that there are two kinds of NiO species. The peak at a lower temperature is assigned to the NiO species interacting weakly with support, and the peak at the higher temperature is attributed to a complex NiO species interacting more strongly with the support [28].

TPR measurements of the different supports were executed to determine the use of Ce in improving the storage capacity and mobility of oxygen. Fig. 11 shows the TPR profiles of the

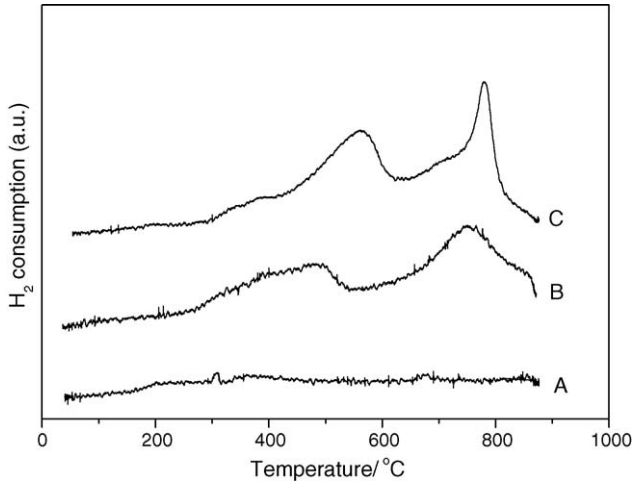

Fig. 11. TPR profiles of the different catalyst supports: (A) TiO_2-700 °C; (B) CeO_2-700 °C; (C) $Ce_{0.50}Ti_{0.50}O_2$-700 °C.

supports, TiO_2, CeO_2, and $Ce_{0.50}Ti_{0.50}O_2$ calcined at 700 °C. No distinct reduction peak was observed in the TiO_2 support. The reduction profile of CeO_2 showed two peaks. The first, low-temperature, signal located at 500 °C was assigned to the reduction of surface-capping oxygen of ceria, while removal of the bulk oxygen was suggested as the cause of the high-temperature signal at 750 °C [29]. And the $Ce_{0.50}Ti_{0.50}O_2$ presented similar reduction peaks, but both these two peaks shifted to higher temperature. Also, the peak area was larger than for CeO_2. The calculated area (per mol of Ce) of the low-temperature peak is 3.7 times larger for $Ce_{0.50}Ti_{0.50}O_2$ than for CeO_2, and the high-temperature peak is 2.5 times larger for $Ce_{0.50}Ti_{0.50}O_2$ than for CeO_2. That is to say, the addition of Ti promotes the reduction of the surface CeO_2 and bulk CeO_2, which can form more bulk oxygen vacancies. The results can help us to confirm that the storage capacity and mobility of oxygen has been improved after the Ti^{4+} enter the ceria lattice.

At the same time, the H_2 consumption of the reduction peak of ceria is different with the various Ce/Ti in Fig. 8. Assigning to the peak area of the ceria reduction in NiO/CeO_2 a value of 1, we calculated the area of this reduction peak (per mol of Ce) in the other catalysts: $NiO/Ce_{0.75}Ti_{0.25}O_2$ is 1.3, $NiO/Ce_{0.50}Ti_{0.50}O_2$ is 2.8, and in $NiO/Ce_{0.25}Ti_{0.75}O_2$ is 2.0. This means that the storage capacity of oxygen has been improved not only in the support ($Ce_{0.50}Ti_{0.50}O_2$), but also in the Ni/Ce-Ti-O catalyst, which is good for resistance to carbon deposition.

3.6. DTA/TG results

As mentioned above, the formation of CeO_2-TiO_2 solid solution improved the storage of oxygen. And the oxygen vacancies of the support could resist the carbon deposition [30]. Information about this aspect was deduced from the thermogravimetric weight gain measurement by comparing measured values with the theoretical weight gain for probable oxidation reaction. DTA/TG analyses of the reduced (fresh catalyst was reduced in 5 vol.% H_2–Ar at 650 for 30 min) and used (after 100 h on stream stability testing) 10 wt.% $NiO/Ce_{0.50}Ti_{0.50}O_2$-700 °C catalyst were carried out in a dry-air atmosphere using a heating rate of 10 °C min^{-1}. Fig. 12 depicts the DTA/TG curves of the samples. There is a broad exothermic peak around 330 °C both in the reduced and used catalysts. TG curve of reduced catalyst shows a weight gain of approximately 2%, which is very close to the theoretical weight gain of Ni to NiO, 2.2%. And the reduced temperature (650 °C) makes it more reasonable. On the contrary, the used catalyst presents a two steps weight gain, which indicates that some other species have been oxidated. Meanwhile, the total weight gain is 2.9%, so it could not be the oxidation of Ni only. In the used catalyst, besides Ni, there is only Ce^{3+} could be oxidated, and the oxidation of Ce^{3+} is easier than Ni. Therefore, we presume that the first step of weight gain (about 0.6%) is due to the Ce^{3+} to Ce^{4+} oxidation; the second step of weight gain (about 2.1%) is due to the Ni^0 to Ni^{2+} oxidation. Meanwhile, there is no obvious weight loss of carbon in these two samples, which means that there is less or no carbon deposit during 100 h on stream testing. These results imply that there are plenty of oxygen vacancies in the used catalyst, which can resist

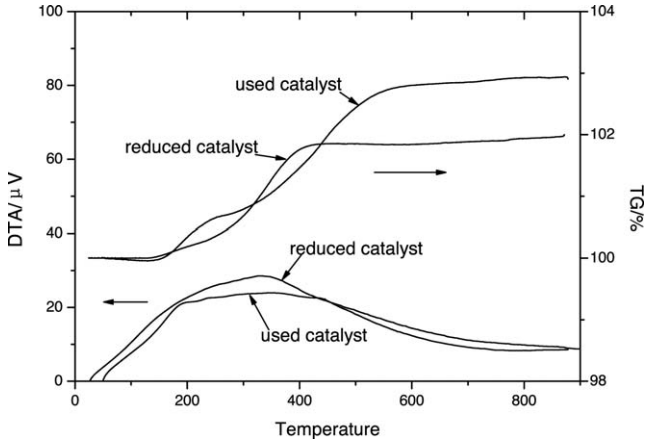

Fig. 12. DTA/TG analysis of reduced and used 10 wt.% $NiO/Ce_{0.50}Ti_{0.50}O_2$-700 °C catalyst.

carbon deposition, and from another point of view, explains the high stability of the catalyst. And it is noticeable that the starting temperature of the second-step weight gain of the used catalyst is 350 °C, which is higher than the reduced one, 170 °C. That may be because the sintering of nickel during the high-temperature catalytic performance testing.

Dong et al. [31] studied the mechanism over Ni/CeO_2, Ni/ZrO_2, and Ni/Ce-ZrO_2 catalysts. They found that the addition of ceria to zirconia enhanced the activity of the catalyst for CH_4 dissociation and improved the carbon storage capacity. Moreover, it increased the storage capacity and mobility of oxygen in the catalyst, thus promoting carbon elimination. Roh et al. [17] discovered that the presence of ceria in the Ni/Ce-ZrO_2 catalyst had beneficial effects on the catalyst performance such as improving the catalyst stability and enhancing concentration of the highly mobile oxygen species. And the interaction between zironia and ceria led to the easier reduction of ceria. For the Ni/Ce-TiO_2 catalyst, it is similar to the Ni/Ce-ZrO_2 catalyst in increasing the storage capacity and mobility of oxygen, which promotes the resistance to carbon deposition. But there is a solid-state reaction between NiO and TiO_2 during the calcination, forming $NiTiO_3$ in the fresh catalyst. After being reduced, the Ni^0 which reduced from $NiTiO_3$ is the active component for POM reaction. While the active component in Ni/Ce-ZrO_2 is the Ni^0 which reduced from the NiO interacted with the support.

4. Conclusions

NiO/Ce-Ti-O catalysts prepared by coprecipitation–impregnation method show a high activity and stability for partial oxidation of methane at the temperature range of 650 to 850 °C. 10 wt.% $NiO/Ce_{0.50}Ti_{0.50}O_2$-700 °C exhibited the highest CH_4 conversion and H_2 selectivity among the catalysts tested, and maintained them during 100 h on stream. XRD and TPR results indicate that the NiO species are well dispersed in the catalysts of NiO/Ce-Ti-O, while bulk NiO particles are just presented in NiO/CeO_2. The solid-state reaction between TiO_2 and NiO is observed in all catalysts containing TiO_2, which leads to the formation of $NiTiO_3$. The formation of ceria-titania

solid solution, which might weaken the interaction of NiO and TiO_2 and have an influence on catalytic stability for the POM reaction, was confirmed by XRD analysis. The solution of Ti^{4+} into ceria (forming solid solution) elevates the oxygen storage capacity, and improves the resistance to carbon deposition. It is shown that Ni^0 reduced from $NiTiO_3$ is active for POM.

Acknowledgement

The financial support of this work by National Natural Science Foundation of China is gratefully acknowledged (No. 20476079).

References

[1] C. Song, Fuel processing for low-temperature and high-temperature fuel cells: challenges, and opportunities for sustainable development in the 21st century, Catal. Today 77 (2002) 17–49.
[2] S.G. Chalk, James.F. Miller, Fred.W. Wagner, Challenges for fuel cells in transport applications, J. Power Sources 86 (2000) 40–51.
[3] N.P. Siegel, M.W. Ellis, D.J. Nelson, M.R. von Spakovsky, Single domain PEMFC model based on agglomerate catalyst geometry, J. Power Sources 115 (2003) 81–89.
[4] M.A. Pena, J.P. Gomez, J.L.G. Fierro, New catalytic routes for syngas and hydrogen production, Appl. Catal. A 144 (1996) 7–57.
[5] S. Freni, G. Calogero, S. Cavallaro, Hydrogen production from methane through catalytic partial oxidation reactions, J. Power Sources 87 (2000) 28–38.
[6] D.A. Hickman, L.D. Schmidt, Synthesis gas formation by direct oxidation of methane over Pt monoliths, J. Catal. 138 (1992) 267–282.
[7] A.K. Bhattacharya, J.A. Breach, S. Chand, Selective oxidation of methane to carbon monoxide on supported palladium catalyst, Appl. Catal. A 80 (1992) L1–L5.
[8] E. Ruckenstein, H.Y. Wang, Effect of support on partial oxidation of methane to synthesis gas over supported rhodium catalysts, J. Catal. 187 (1999) 151–159.
[9] K. Walter, O.V. Buyevskaya, D. Wolf, M. Baerns, Rhodium-catalyzed partial oxidation of methane to CO and H_2—in-situ DRIFTS studies on surface intermediates, Catal. Lett. 29 (1994) 261–270.
[10] D.A. Hickman, L.D. Schmidt, Syngas formation by direct catalytic oxidation of methane, Science 259 (1993) 343–349.
[11] L. Basini, A. Aragno, G. Vlaic, Molecular mechanisms in partial oxidation of methane on Ir/alpha-Al_2O_3: reactivity dependence on catalyst properties and transport phenomena limitations, Catal. Lett. 39 (1996) 49–55.
[12] Q.G. Yan, T.H. Wu, W.Z. Weng, H. Toghiani, R.K. Toghiani, H.L. Wan, C.U. Pittman Jr., Partial oxidation of methane to H_2 and CO over Rh/SiO_2 and Ru/SiO_2 catalysts, J. Catal. 226 (2004) 247–259.
[13] A.F. Ghenciu, Review of fuel processing catalysts for hydrogen production in PEM fuel cell systems, Curr. Opin. Solid State Mater. 6 (2002) 389–399.
[14] A.M. Diskin, R.H. Cunningham, R.M. Ormerod, The oxidative chemistry of methane over supported nickel catalysts, Catal. Today 46 (1998) 147–154.
[15] T. Wu, Q. Yan, H. Wan, Partial oxidation of methane to hydrogen and carbon monoxide over a Ni/TiO_2 catalyst, J. Mol. Catal. A: Chem. 226 (2005) 41–48.
[16] T. Zhu, M. Flytzani-Stephanopoulos, Catalytic partial oxidation of methane to synthesis gas over Ni-CeO_2, Appl. Catal. A208 (2001) 403–417.
[17] H.S. Roh, W.S. Dong, K.W. Jun, S.E. Park, Partial oxidation of methane over Ni catalysts supported on Ce-ZrO_2 mixed oxide, Chem. Lett. 205 (2001) 88–89.
[18] T. Takeguchi, S. Furukawa, M. Inoue, Hydrogen spillover from NiO to the large surface area CeO_2-ZrO_2 solid solutions and activity of the NiO/CeO_2-ZrO_2 catalysts for partial oxidation of methane, J. Catal. 202 (2001) 14–24.
[19] E. Mamontov, T. Egami, Structural defects in a nano-scale powder of CeO_2 studied by pulsed neutron diffraction, J. Phy. Chem. Solids 61 (2000) 1345–1356.
[20] S. Tang, J. Lin, K.L. Tan, Partial oxidation of methane to syngas over Ni/MgO, Ni/CaO and Ni/CeO_2, Catal. Lett. 51 (1998) 169.
[21] T. López, F. Rojas, R. Alexander-Katz, F. Galindo, A. Balankin, A. Buljan, Porosity, structural and fractal study of sol–gel TiO_2-CeO_2 mixed oxides, J. Solid State Chem. 177 (2004) 1873–1885.
[22] J. Rynkowski, J. Farbotko, R. Touroude, L. Hilaire, Redox behavior of ceria-titania mixed oxides, Appl. Catal. A 203 (2000) 335–348.
[23] M.S.P. Francisco, V.R. Mastelaro, Activity and characterization by XPS, HR-TEM, Raman Spectroscopy, and BET surface area of CuO/CeO_2-TiO_2 catalysts, J. Phys. Chem. B 105 (2001) 10515–10522.
[24] R. Jenkins, R.L. Snyder, Introduction to X-ray Diffractometry, Wiley, New York, 1996.
[25] R. Molina, G. Poncelet, α-Alumina-supported nickel catalysts prepared from nickel acetylacetonate: a TPR study, J. Catal. 173 (1998) 257–267.
[26] J.A. Montoya, E. Romero-Pascual, C. Gimon, Methane reforming with CO_2 over Ni/ZrO_2-CeO_2 catalysts prepared by sol–gel, Catal. Today 63 (2000) 71–85.
[27] S. Pengpanich, V. Meeyoo, T. Rirksomboon, Methane partial oxidation over Ni/CeO_2-ZrO_2 mixed oxide solid solution catalysts, Catal. Today 93–95 (2004) 95–105.
[28] H.S. Roh, K.W. Jun, W.S. Dong, J.S. Chang, S.E. Park, Y. Joe, Highly active and stable Ni/Ce-ZrO_2 catalyst for H_2 production from methane, J. Mol. Catal. A: Chem. 181 (2002) 137–142.
[29] F. Giordano, A. Trovarelli, C. Leitenburg, M. Giona, A model for the temperature-programmed reduction of low and high surface area ceria, J. Catal. 193 (2000) 273–282.
[30] E. Ramírez-Cabrera, A. Atkinson, D. Chadwick, The influence of point defects on the resistance of ceria to carbon deposition in hydrocarbon catalysis, Solid State Ionics 136–137 (2000) 825–831.
[31] W.S. Dong, K.W. Jun, H.S. Roh, Z.W. Liu, S.E. Park, Comparative study on partial oxidation of methane over Ni/ZrO_2, Ni/CeO_2 and Ni/Ce-ZrO_2 catalysts, Catal. Lett. 78 (2002) 215–222.